ISSN 0021-8944, Journal of Applied Mechanics and Technical Physics, 2021, Vol. 62, No. 4, pp. 624–632. © Pleiades Publishing, Ltd., 2021.
Russian Text © O.I. Gusev, G.S. Khakimzyanov, L.B. Chubarov, D. Dutykh.

ASSESSING THE FREQUENCY DISPERSION INFLUENCE ON THE SOLITARY-WAVE INTERACTION WITH A CONSTANT SLOPING BEACH

O. I. Gusev[a,b], **G. S. Khakimzyanov**[a,b], **L. B. Chubarov**[a,b,*], **and D. Dutykh**[c]

UDC 532.5+519.63

Abstract: This article focuses on the effect of frequency dispersion on the wave run-up height and the characteristics of the surface waves reflected from a coastal slope. Calculations are performed within the framework of nonlinear dispersive and nondispersive shallow water models using the original boundary conditions on a moving shoreline. A case study of the problem of solitary wave run-up on flat coastal slopes with parameters close to the characteristics of one of the Kamchatka bays shows that the nondispersive model overestimates the maximum run-up and amplitudes of the reflected waves by 10–20%.

Keywords: surface waves, shoreline, coastal run-up, nonlinear dispersive shallow water equations, shoreline boundary conditions, numerical modeling.

DOI: 10.1134/S0021894421040118

INTRODUCTION

Paper [1] dealing with the assessment of the impact of long surface waves on partially submerged structures (floating nuclear power plants, liquefied gas storage tanks) was presented at the Nonlinear Waves—2021 All-Russian conference dedicated to the 75th anniversary of Corresponding Member of RAS V. M. Teshukov. Since, in some cases, such structures have to be placed in tsunami-prone coastal areas, they should be designed and operated taking into account the possible catastrophic impact of long surface waves. Recently, there has been an increase in research effort in this area. Along with laboratory experiments [2, 3] and analytical methods, numerical modeling methods are widely used to determine the characteristics of interaction of waves with semi-submerged large structures. Much attention has been paid to the study of maximum run-up on a structure and the characteristics of waves reflected from it and passing over it (in Fig. 1, the wave reflected from the beach is shown by line *2*). However, insufficient attention has been given to the impact of waves reflected from the beach on such structures, which in some cases is at least comparable to the impact of incident waves (line *1* in Fig. 1).

[a]Federal Research Center for Information and Computing Technologies, Novosibirsk, 630090 Russia. [b]Novosibirsk National Research State University, Novosibirsk, 630090 Russia. [c] Univ. Grenoble Alpes, Univ. Savoie Mont Blanc, CNRS, LAMA, 73000 Chambéry, France; gusev_oleg_igor@mail.ru, khak@ict.nsc.ru, *chubarovster@gmail.com, denys.dutykh@gmail.com. Translated from Prikladnaya Mekhanika i Tekhnicheskaya Fizika, Vol. 62, No. 4, pp. 114–123, July–August, 2021. Original article submitted April 20, 2021; revision submitted April 20, 2021; accepted for publication April 26, 2021.

*Corresponding author.

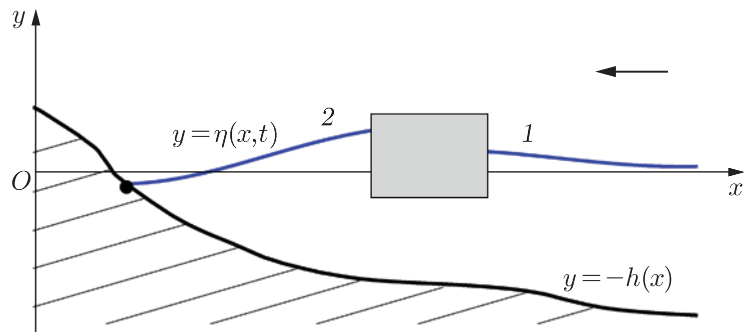

Fig. 1. Position of the free boundary $y = \eta(x, t)$ at the time when the incident wave (*1*) has passed over the semi-submerged structure and a wave reflected from the beach formed (*2*): the point is a shoreline point which moves along the beach slope $y = -h(x)$, and the arrow shows the direction of the incident wave.

Paper [4] presents formulations of problems of interaction of long surface waves with semi-submerged structures within a hierarchy of models that includes shallow water models, in particular, the fully nonlinear dispersive Serre–Green–Naghdi (SGN) model of the second long-wave approximation [5] and the nondispersive shallow water model of nonlinear shallow water equations (NSWE model) of the first approximation.

The practical significance of the hierarchical approach lies not only in increasing the reliability of modeling results by using higher-order approximation models, but also in a significant saving in computational time of multivariate calculations through the use of less costly algorithms based on lower-order models in cases where they provide the necessary accuracy.

As is known, the solution of problems of wave run-up on a beach is greatly complicated by the mobility of the shoreline — the water–land interface. This interface is not known in advance and must be determined, together with other required quantities, during the calculation. The shock-capturing method in a fixed domain with fixed boundaries [6] using different procedures to track the moving shoreline [7–9] is the most common method for calculating the wave–beach interaction with the framework of shallow water models. In this method, the position of the water–land interface is approximately determined by analyzing the calculated values of the total depth.

When using the method in which the shoreline is explicitly identified, the shallow water equations are solved only in the region occupied by water, and numerical algorithms should take into account the time variation of the solution domain due to the mobility of the shoreline (see, e.g., [10, 11]). Within the framework of dispersive shallow water models, this method has not previously been used due to the difficulty of formulating moving shoreline boundary conditions and due to the absence of proof of the need to take into account the dispersion of waves during run-up on the shore, since it is assumed that in the case of long waves, dispersion effects can manifest themselves only during prolonged propagation [12]. However, a study [13] of the impact of the Tohoku tsunami (2011) on breakwater structures near the city of Soma (Japan) has shown that the impact of an undular bore on nearshore breakwaters cannot be modeled without taking into account dispersion.

Under certain conditions, the breaking of waves running on a beach is possible. Original nonlinear dispersive models and numerical algorithms that reproduce near-shore wave breaking with high accuracy are proposed in [14, 15].

In the present paper, the run-up of surface waves on a beach is calculated using the one-dimensional SGN model with explicit identification of a moving shoreline point. Formulas for calculating the trajectory and velocity of the shoreline point are derived using the technique previously employed for the NSWE equations [16]. The effect of wave dispersion on wave run-up on a flat slope and on the formation of waves reflected from it is assessed. For this, the calculation results using the SGN model and the nondispersive NSWE model are compared.

The modeling of wave run-up on a beach is considered as an independent methodological problem not related to the modeling of wave impact on semi-submerged structures; therefore, the waves incident on the beach (passing the structure) are modeled using solitary waves of a certain amplitude.

1. FORMULATION OF THE PROBLEM FOR THE SGN EQUATIONS

Consider an incompressible inviscid fluid layer bounded by a free surface and an impermeable bottom in a gravitational field. We choose a Cartesian coordinate system Oxy such that the equation for the free surface of the fluid at rest is $y = 0$, and the known function $y = -h(x)$ specifies the relief of the bottom and adjacent land areas. Surface waves are assumed to propagate along the normal to the rectilinear shoreline. Under the above assumptions, the problem of wave run-up on the beach is solved with the framework of the shallow water models in the one-dimensional approximation.

In the SGN model, the desired quantities are the vertically averaged velocity $u(x, t)$ and the total depth $H = \eta + h$, where t is time; $\eta(x, t)$ is the deviation of the free surface from the unperturbed level. Another desired parameter is the abscissa $x_0(t)$ of the shoreline point for $t > 0$, for which

$$\dot{x}_0(t) = U(t) = u(x_0(t), t) \tag{1}$$

($U(t)$ is the velocity of the shoreline point).

We assume that the wave moves along the water area from right to left and, during run-up, the shoreline point moves along the beach slope located on the left side of the area. Thus, the SGN equation must be solved in the domain $\Omega(t) = (x_0(t), l)$ with a moving left boundary on which the following boundary condition is specified:

$$H(x_0(t), t) = 0. \tag{2}$$

On the fixed right boundary $x = l$, we specify the no-flow condition and in the domain $\Omega(0)$, the initial conditions

$$H(x, 0) = H_0(x), \qquad u(x, 0) = u_0(x), \qquad x \in [x_{00}, l],$$

where $x_{00} = x_0(0)$ is the known position of the shoreline point at the initial time.

Let the smooth nondegenerate transformation of coordinates

$$x = x(q, t), \qquad x(0, t) = x_0(t), \qquad x(1, t) = l \tag{3}$$

maps one-to-one the unit segment $\bar{Q} = [0, 1]$ to $\bar{\Omega}(t) = [x_0(t), l]$, J is the Jacobian of this transformation, $J(q, t) = x_q(q, t) \geqslant J_0$, $J_0 = \text{const} > 0$. In the coordinates q and t, the system of one-dimensional equations of the SGN model has the form [5]

$$(JH)_t + [(u - x_t)H]_q = 0; \tag{4}$$

$$(JHu)_t + [(u - x_t)Hu + gH^2/2]_q = gHh_q + \varphi_q - \psi h_q; \tag{5}$$

$$(k\varphi_q)_q - 6\varphi\Big[\frac{2J}{H^3}\,\frac{r-3}{r} + \Big(\frac{h_q}{JH^2 r}\Big)_q\Big] = F, \tag{6}$$

where g is the acceleration due to gravity; φ is the dispersive component of the depth-integrated pressure in the SGN model; ψ is the dispersive component of the pressure on the bottom:

$$\psi = \frac{1}{r}\Big(\frac{6\varphi}{H} + HR + \frac{\varphi_q h_q}{J^2}\Big), \quad r = 4 + \frac{h_q^2}{J^2}, \quad R = -g\,\frac{\eta_q h_q}{J^2} + u^2\,\frac{1}{J}\Big(\frac{h_q}{J}\Big)_q,$$

$$k = \frac{4}{JHr}, \qquad F = \Big(g\,\frac{\eta_q}{J} + \frac{Rh_q}{Jr}\Big)_q - \frac{6RJ}{Hr} + 2\,\frac{u_q^2}{J}.$$

In the split system of equations (4)–(6), the desired quantities are the velocity $u(q, t)$, the total depth $H(q, t)$, the position of the shoreline $x_0(t)$, and the dispersive pressure component $\varphi(q, t)$.

Conversion to a new coordinate system allows the problem to be solved in the domain Q with fixed boundaries. An analog of condition (2) is the boundary condition

$$H(0, t) = 0, \tag{7}$$

which leads to two boundary conditions

$$\varphi(0, t) = 0; \tag{8}$$

$$\Big(k\varphi_q - \frac{6h_q}{JH^2 r}\,\varphi\Big)\Big|_{q=0} = \dot{U}(t) + \Big(\frac{1}{J}\,g\eta_q + \frac{R}{Jr}\,h_q\Big)\Big|_{q=0}, \tag{9}$$

which are used separately in successive steps of the numerical algorithm of solution of Eq. (6). On the right boundary $q = 1$, we use the no-flow condition $u(1,t) = 0$ and its associated boundary condition for the dispersive component φ:

$$\Big(k\varphi_q - \frac{6h_q}{JH^2 r}\,\varphi\Big)\Big|_{q=1} = \Big(\frac{1}{J}\,g\eta_q + \frac{R}{Jr}\,h_q\Big)\Big|_{q=1}.$$

The nondispersive shallow water NSWE equations follow from Eqs. (4) and (5) if in the latter we set $\varphi \equiv 0$ and $\psi \equiv 0$.

2. SOLUTION METHOD

For the numerical solution of the problem of wave run-up on a beach, we use a modified version of the predictor/corrector scheme [5] developed for numerical investigation of fluid flows with surface waves in water areas with fixed boundaries. In this scheme, the system of hyperbolic equations (4) and (5) and Eq. (6) are solved alternately in both the predictor and corrector steps; the values of the grid functions calculated in the previous steps of the computational algorithm are used on the right-hand sides of the equations and in the expressions for the coefficients of the difference equations. The modified scheme can be used to solve problems in a domain with a moving boundary coinciding with the shoreline point.

2.1. Law of Motion of the Shoreline Point

Suppose that at the time $t = t^n$, the adaptive grid $\{x_j^n\}$ $(j = 0, \ldots, N)$, the velocity u_j^n, the free boundary η_j^n, the dispersive pressure component φ_j^n, and the position of the shoreline point are known and $x_0^n = x_0(t^n)$, $u_0^n = U(t^n)$, $H_0^n = 0$. To determine these quantities at the next time layer $t^{n+1} = t^n + \tau$, we first calculate the new position of the shoreline point $x_0(t^{n+1})$ and its velocity $U(t^{n+1})$ using boundary condition (7), its consequences $H_t(0,t) = 0$ and $H_{tt}(0,t) = 0$, and the assumptions that Eqs. (4) and (5) are valid in the entire computational domain up to the left boundary $q = 0$, and the initial data for these equations are given at $t = t^n$ by functions of the continuous argument q:

$$u(q,t^n) = u^n(q), \qquad H(q,t^n) = H^n(q), \qquad q \in \bar{Q}. \tag{10}$$

The form of the expressions for the trajectory of the shoreline point $x_0(t)$ and its velocity $U(t)$ depends on the slope of the free boundary at the point of its intersection with the beach slope. In the case of the strict inequality (mode 1)

$$H_q^n(0) > 0 \tag{11}$$

the law of motion of the shoreline point is uniquely determined from condition (2) [16], and the trajectory $x = x_0(t)$ of the shoreline point can be sought at $t \geqslant t^n$ in the form of the power series in time

$$x_0(t) = x_0^n + x_{01}(t - t^n) + x_{02}(t - t^n)^2/2 + x_{03}(t - t^n)^3/6 + O((t - t^n)^4). \tag{12}$$

Equality (1) implies that

$$U(t) = x_{01} + x_{02}(t - t^n) + x_{03}(t - t^n)^2/2 + O((t - t^n)^3), \tag{13}$$

whence we obtain $x_{01} = U(t^n) = u_0^n$, i.e., the coefficient x_{01} is equal to the value of the known fluid velocity at the shoreline point at the time $t = t^n$.

Using the method of [16], the remaining coefficients x_{0k} $(k \geqslant 2)$ can also be expressed in terms of the initial data (10) for an arbitrary shape of the beach slope. We give the formulas only for x_{02} and x_{03}, which correspond to the beach slope adjacent on the right to a region of constant depth h_0:

$$y = -h(x) = \begin{cases} y_0 - x\tan\theta, & 0 \leqslant x \leqslant x_s, \\ -h_0, & x_s < x \leqslant l, \end{cases} \tag{14}$$

where $\theta > 0$ is the slope of the beach; $y_0 > 0$ is the height of the land area at the point $x = 0$; $x_s = (y_0 + h_0)\cot\theta$ is the abscissa corresponding to the base of the slope. For this bottom shape, the following formulas for the first coefficients of series (12) and (13) are valid:

$$x_{01} = u_0^n, \quad x_{02} = -g(1 + \eta_x^n \tan\theta)\eta_x^n\Big|_{x=x_0^n}, \quad x_{03} = 2g(1 + 2\eta_x^n \tan\theta)u_x^n H_x^n\Big|_{x=x_0^n}. \tag{15}$$

The coefficients x_{02} and x_{03} for the nondispersive NSWE model are calculated by formulas different from (15):

$$x_{02} = -g\eta_x^n\Big|_{x=x_0^n}, \qquad x_{03} = 2gu_x^n H_x^n\Big|_{x=x_0^n}. \tag{16}$$

For the second possible case (mode 2)

$$H_q^n(0) = 0, \tag{17}$$

where the tangent to the free boundary at the shoreline point at the time $t = t^n$ coincides with the tangent to the bottom surface, the law of motion of the shoreline point is obtained by solving the system of two ordinary differential equations

$$\begin{gathered} \dot{x}_0(t) = U(t), \qquad t > t^n, \\ \dot{U}(t) = \left[g - g\Big(\frac{h_q}{J}\Big)^2 - U^2(t)\,\frac{1}{J}\Big(\frac{h_q}{J}\Big)_q\right]\frac{h_q}{J}\Big|_{q=0}, \qquad t > t^n \end{gathered} \tag{18}$$

with the initial conditions

$$x_0(t^n) = x_0^n, \qquad U(t^n) = u_0^n. \tag{19}$$

In the case of a flat slope (14), problem (18), (19) has the exact solution

$$\begin{gathered} x_0(t) = x_0^n + u_0^n(t - t^n) + g(1 - \tan^2\theta)\tan\theta\,(t - t^n)^2/2, \\ U(t) = u_0^n + g(t - t^n)(1 - \tan^2\theta)\tan\theta. \end{gathered} \tag{20}$$

For the NSWE model, the exact solution is given by the formulas

$$\begin{gathered} x_0(t) = x_0^n + u_0^n(t - t^n) + g\tan\theta\,(t - t^n)^2/2, \\ U(t) = u_0^n + g\tan\theta\,(t - t^n). \end{gathered} \tag{21}$$

The form of the obtained relations for determining the position and velocity of the moving shoreline point depends on the mode of wave–shore interaction. In the numerical calculations, the mode is determined in accordance with the value of the difference derivative $H_{x,0}^n$ at the node x_0^n. If this derivative satisfies the condition

$$H_{x,0}^n \geqslant \delta_H,$$

it is assumed that the first mode occurs (see (11)), and if it satisfies the condition

$$H_{x,0}^n < \delta_H \text{ —}$$

the second mode occurs (see (17)) ($\delta_H > 0$ is a given small parameter, whose optimal value depends on the grid step size in the computational domain and the flow characteristics in the vicinity of the shoreline point).

2.2. *Computational Algorithm*

After the new position of the shoreline point $x_0(t^{n+1})$ and its velocity $U^{n+1} = U(t^{n+1})$ are found, a new grid $\{x_j^{n+1}\}$ $(j = 0, \ldots, N)$ is constructed, whose nodes at the time t^{n+1} are the images obtained by mapping (3) of the nodes of the fixed uniform grid $\{q_j\}$ covering the computational domain $\bar{Q}$ [5]. The left node x_0^{n+1} of the moving grid coincides with the shoreline point, and the values of all the desired quantities at this node were already calculated or determined from the boundary conditions

$$u_0^{n+1} = U^{n+1}, \qquad H_0^{n+1} = 0, \qquad \varphi_0^{n+1} = 0.$$

At the other nodes, these quantities are calculated using the predictor/corrector scheme with the same algorithms [5] of solution of Eqs. (4), (5) for the SGN and NSWE models. When using the SGN model to determine the dispersive pressure component, Eq. (6) is additionally solved. Boundary condition (9) is used in the predictor step, and condition (8) in the corrector step.

3. NUMERICAL SIMULATION RESULTS

A model problem with bottom relief (14) in the form of a flat horizontal section adjacent to a flat slope is investigated. The initial data at $t = 0$ are taken to be the solitary wave

$$\eta_0(x) = a_0 \operatorname{sech}^2\Big(\frac{\sqrt{3a_0 g}}{2U_0}\,\frac{x - x_w}{h_0}\Big), \qquad H_0(x) = h(x) + \eta_0(x),$$
$$u_0(x) = -U_0\,\frac{\eta_0(x)}{h_0 + \eta_0(x)}, \tag{22}$$

where $x \in [x_{00}, l]$; a_0 is the wave amplitude; x_w is the abscissa of the crest of the wave; $U_0 = \sqrt{g(h_0 + a_0)}$. In formula (14) the quantity $y_0/h_0 = 1$ is chosen in such a way

that the maximum vertical run-up of the wave on the beach slope does not exceed this value.

At the initial time, the crest of the wave (22) was located at a sufficient distance from the base of the slope x_s, which guaranteed that most of the initial wave was above the horizontal part of the bottom. Note that for the case of constant depth h_0 and initial data (22), the SGN equations have an exact solution in the form of a soliton moving without a change in its initial shape to the left with velocity U_0. The NSWE equations have no soliton solution, and in the case of motion over the horizontal bottom for a long time, the shape of the wave is significantly different from the initial shape. Therefore, to study the interaction of the least

deformed solitary wave with the slope, it must be placed almost close to the base of the slope, e.g., in the following manner:

$$x_w = x_s + \lambda/2.$$

Here λ is the effective wavelength equal to the distance between two points of the wave surface that are symmetric about the wave crest and at which the wave height is fraction Π of the amplitude a_0:

$$\eta_0(x_w \pm \lambda/2) = a_0\Pi.$$

From this we obtain

$$\lambda = 4h_0\sqrt{\frac{a_0 + h_0}{3a_0}}\,\ln\Big(\sqrt{\frac{1}{\Pi}} + \sqrt{\frac{1}{\Pi} - 1}\Big).$$

In the calculations, we used a value $\Pi = 0.05$.

At $t = 0$, the abscissa x_{00} was determined from the equation $\eta_0(x)+h(x) = 0$. The length of the domain l was specified so as to minimize the influence of the boundary conditions on the right boundary of the computational domain on the characteristics of wave run-up on the slope: $l = x_s + 100h_0$. The values $h_0 = 42$ m, $a_0 = 3$ m were chosen close to the values of the parameters of one of the Kamchatka bays, for which probabilistic estimates of tsunami hazard with an average repeatability of once per 100 years were obtained earlier. The slope angle θ was in the range 4–15°.

We investigate the transformation of the wave during interaction with the slope. Figure 2 shows the free surface at a slope angle $\theta = 4°$ calculated using the SGN model. The beginning of the process involves the formation of a small-amplitude wave reflected from the base of the slope, which propagates in the opposite direction (to the right). The leading edge of the main wave moving along the slope becomes steeper.

The trajectories of the shoreline point for angles $\theta = 4$, 8, 12° calculated using the SGN and NSWE models are shown in Fig. 3. It is seen that as the slope angle decreases, the trajectory becomes more complicated, the number of run-up and backwash phases and the backwash height increase (see also Fig. 4a). In all cases, the maximum run-up height calculated using the NSWE model is approximately 10–20 % larger than that determined taking into account the frequency dispersion (SGN model), and for the backwash depth, the situation is opposite. Note that as the slope angle decreases, on the one hand, the distance and time of travel of the wave along the slope increase, resulting in an increase in the influence of dispersion effects, and on the other hand, the difference of the positions and velocities of the shoreline point calculated by formulas (15), (20) (SGN model) and (16), (21) (NSWE model) decreases.

During backwash, a train of waves of smaller amplitude is formed behind the leading wave. It is clearly seen in the records of the virtual tide gauge located at the point x_w and on the calculated free-surface profiles

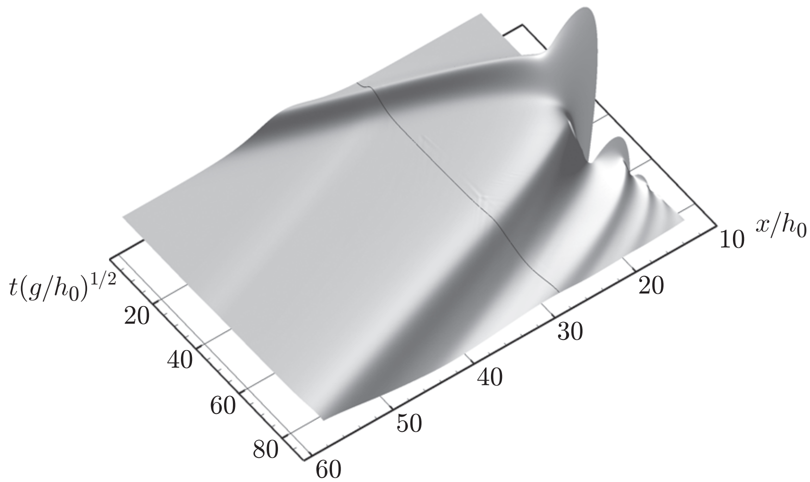

Fig. 2. Shape of the free surface of the wave interacting with a flat slope ($\theta = 4°$) obtained using the SGN model: the solid curved shows the position of the beginning of the slope.

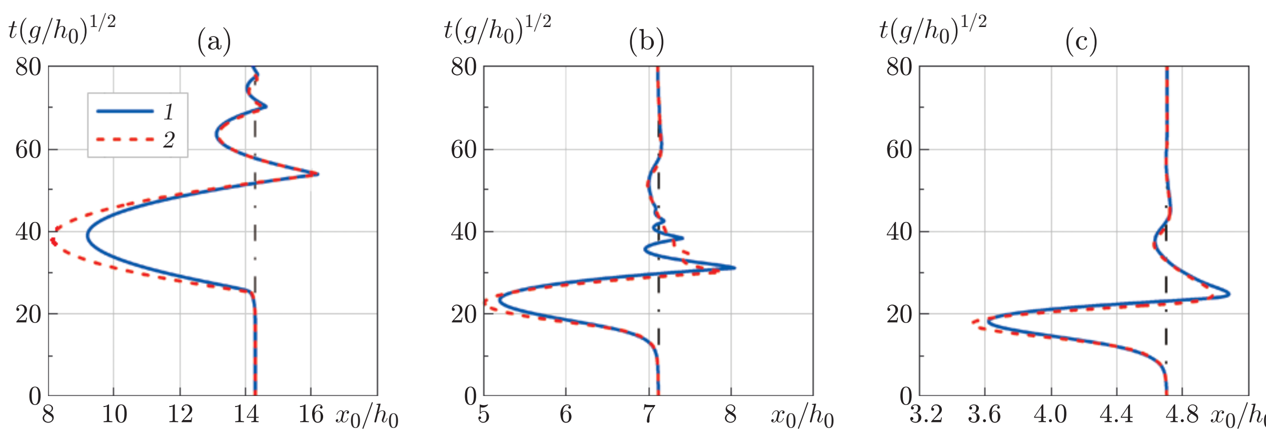

Fig. 3. Trajectories of the shoreline point calculated using the SGN model (*1*) and the NSWE model (*2*) for various slope angles: (a) $\theta = 4°$, (b) $\theta = 8°$, (c) $\theta = 12°$.

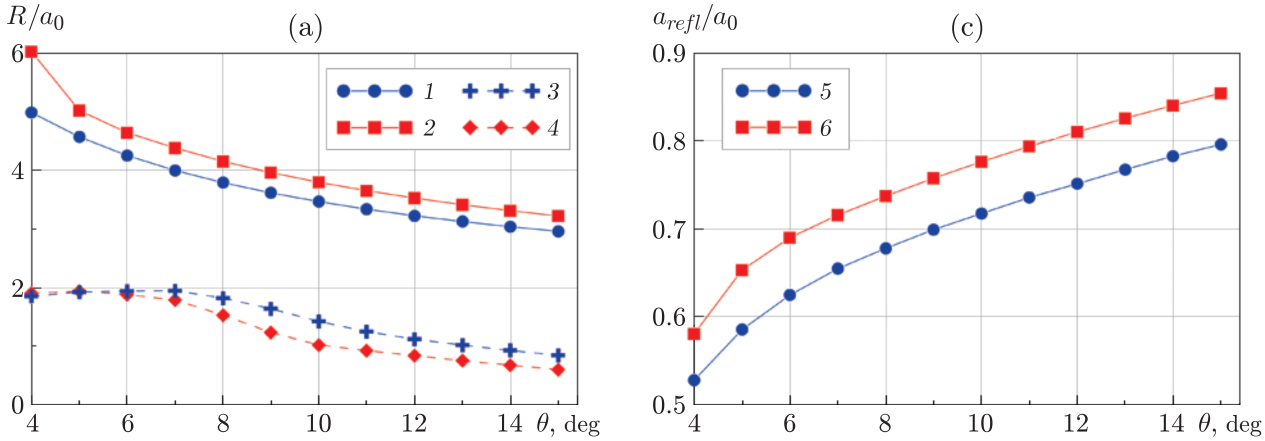

Fig. 4. Dependences of the maximum run-up height (*1, 2*), backwash depth (*3, 4*) (a), and reflected wave amplitude (*5, 6*) (b) on the angle slope calculated using the SGN model (*1, 3, 5*) and the NSWE model (*2, 4, 6*).

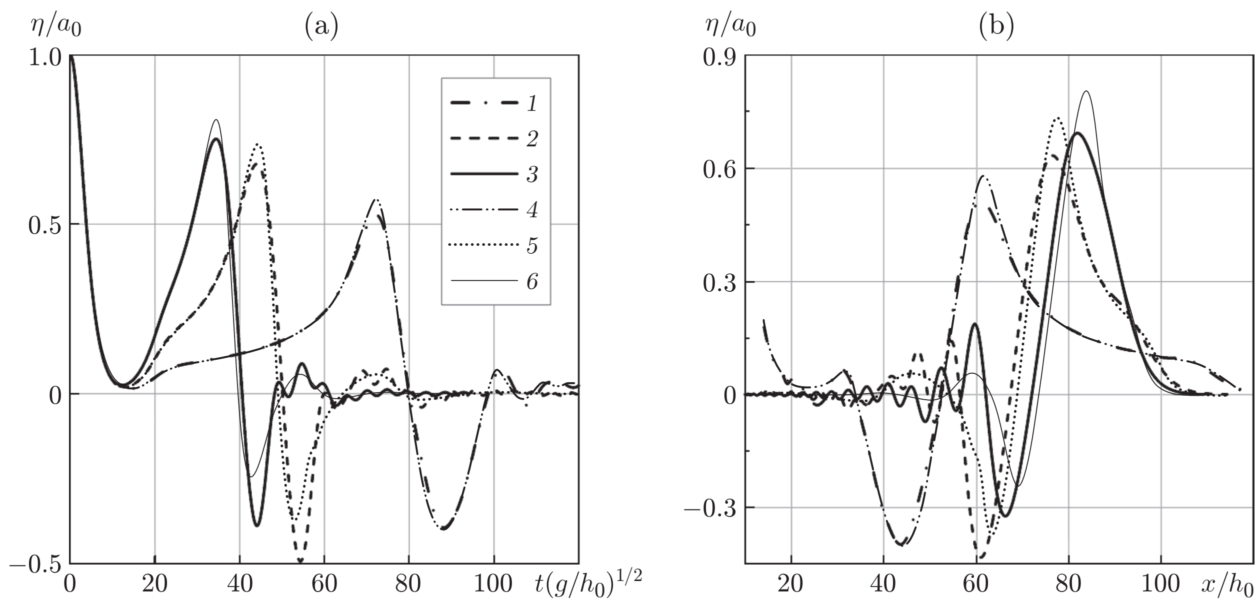

Fig. 5. Free-surface profiles obtained using a virtual tide gauge located at the point x_w (a) and calculated for the time $t\sqrt{g/h_0} = 94$ (b): (*1–3*) SGN model, (*4–6*) NSWE model; (*1, 4*) $\theta = 4°$, (*2, 5*) $\theta = 8°$, and (*3, 6*) $\theta = 12°$.

at the time $t\sqrt{g/h_0} = 94$ (Fig. 5). With decreasing slope angle, the maximum amplitude of the reflected wave decreases in such a way that the values obtained using the NSWE model become larger than those calculated using the SGN model (Fig. 4b). The height of the reflected wave (the difference of the maximum magnitudes of positive and negative deviations of the free surface during successive oscillations) calculated using the SGN model turns out to be larger than that calculated using the NSWE model; therefore, the impact on the semi-submerged structure may also be larger.

CONCLUSIONS

The boundary conditions at a moving shoreline point were formulated for the completely nonlinear dispersive shallow water model of the second approximation. The influence of dispersion effects during run-up and formation of waves reflected from a mild sloping beach with different slope angles were determined. It was shown that with dispersion taken into account, the maximum run-up height and distance and the amplitude of the reflected wave decrease by 10–20 %. With an increase in the slope angle, the backwash depth and the height of the reflected waves increase.

The identified regularities and the proposed analytical and algorithmic constructs can be used to improve the accuracy of modeling the interaction of long waves with semi-submerged structures located near beach slopes.

In the future, it is planned to consider more realistic bottom relief and shapes of waves approaching a beach to model the interaction of waves not only with a beach slope, but also with semi-submerged structures located near the shoreline taking into account other important factors, e.g., bottom friction.

The work has been supported by State assignment of the Federal Research Center for Information and Computational Technologies and by the French National Research Agency through the Investments for Future Program (No. ANR-18-EURE-0016 — Solar Academy); the work presented in the Solution Method Section was supported by the Russian Scientific Foundation (Grant No. 21-71-00127).

REFERENCES

1. O. I. Gusev, G. S. Khakimzyanov, and L. B. Chubarov, "Numerical Investigation of the Impact of Long Surface Waves on a Partially Submerged Fixed Non-Deformable Structure,"in *Nonlinear waves—2021: All-Russian. Conf. with Int. Participation dedicated to the 75th anniversary of Corresponding Member of RAS V. M. Teshukov*, Novosibirsk, March 2–4, 2021, p. 27. http://conf.nsc.ru/files/conferences/nw2021/625257/abstract.pdf.
2. E. Yu. Kamynin, V. V. Maksimov, I. S. Nudner, et al., "Interaction of a Solitary Wave with a Partially Submerged Fixed Structure," Fund. i Prikl. Gidrofiz., No. 4, 39–54 (2010).
3. X. Lu and K.-H. Wang, "Modeling a Solitary Wave Interaction with a Fixed Floating Body Using an Integrated Analytical-Numerical Approach," Ocean Engng. **109**, 691–704 (2015).
4. G. S. Khakimzyanov and D. Dutykh, "Long Wave Interaction with a Partially Immersed Body. Pt 1. Mathematical Models," Comm. Comput. Phys. **27** (2), 321–378 (2020).
5. G. Khakimzyanov, D. Dutykh, Z. Fedotova, and O. Gusev, "Dispersive Shallow Water Waves. Theory, Modeling, and Numerical Methods," (Birkhäuser, Basel, 2020). (Lecture notes in geosystems mathematics and computing).
6. S. C. Medeiros and S. C. Hagen, "Review of Wetting and Drying Algorithms for Numerical Tidal Flow Models," Intern. J. Numer. Methods Fluids **71**, 473–487 (2013).
7. D. Dutykh, T. Katsaounis, and D. Mitsotakis, "Finite Volume Schemes for Dispersive Wave Propagation and Runup," J. Comput. Phys. **230** (8), 3035–3061 (2011).
8. F. Shi, J. T. Kirby, J. C. Harris, et al., "A High-Order Adaptive Time-Stepping TVD Solver for Boussinesq Modelling of Breaking Waves and Coastal Inundation," Ocean Model. **43/44**, 36–51 (2021).
9. J. P. A. Pitt, C. Zoppou, and S. G. Roberts, "Solving the Fully Nonlinear Weakly Dispersive Serre Equations for Flows over Dry Beds," Intern. J. Numer. Methods Fluids **93**, 24–43 (2021).
10. V. G. Sudobicher and S. M. Shugrin, "Flow of Water in Dry Channels," Izv. SO AN SSSR. Ser. Tekhn. Nauk **13** (3), 116–122 (1968).
11. V. M. Lyatkher and A. N. Militeev, "Calculation of the Run-Up of Long Gravitational Waves on a Slope," Oceanology **14** (1), 37–42 (1974).
12. J. T. Kirby, F. Shi, B. Tehranirad, et al., "Dispersive Tsunami Waves in the Ocean: Model Equations and Sensitivity to Dispersion and Coriolis Effects," Ocean Model. **62**, 39–55 (2013).
13. D. Morichon, V. Roeber, M. Martin-Medina, et al., "Tsunami Impact on a Detached Breakwater: Insights from Two Numerical Models," J. Waterway, Port, Coastal Ocean Engng. **147** (2), 05021001 (2021).
14. S. L. Gavrilyuk, V. Yu. Liapidevskii, and A. A. Chesnokov, "Spilling Breakers in Shallow Water: Applications to Favre Waves and to the Shoaling and Breaking of Solitary Waves," J. Fluid Mech. **808**, 441–468 (2016).
15. M. Kazakova and G. Richard, "A New Model of Shoaling and Breaking Waves: One-Dimensional Solitary Wave on a Mild Sloping Beach," J. Fluid Mech. **862**, 552–591 (2019).
16. S. P. Bautin, S. L. Deryabin, A. F. Sommer, et al., "Use of Analytic Solutions in the Statement of Difference Boundary Conditions on a Movable Shoreline," Russ. J. Numer. Anal. Math. Model. **26** (4), 353–377 (2011).